Effect of deformation temperature on microstructure in coating of galvanized hot-formed steel

Letian Liu[1], Yikang Dong[1,†], Renjie Xue[1], Ze Wang[1], Bo Chen[2], Shuai Song[1] and Lihui Wang[1]

[1]*HBIS Material Technology Research Institute, Shijiazhuang, 050023, China*
[2]*HBIS Automobile Plate Co., Ltd., TianJin, 300000, China*
[†]*E-mail: dongyikang@hbisco.com*

Zinc-based coating hot forming steel has good cathodic protection characteristics, which makes up for the deficiency of corrosion resistance of aluminum-silicon coating products. However, in the process of hot forming, due to the existence of high temperature liquid zinc, it is easy to cause the problem of liquid metal embrittlement, which limits the market promotion and application of the steel. In this paper, based on Gleeble 3800 thermal simulation testing machine, the matrix structure and coating structure of hot-dip galvanized hot forming steel at different deformation temperatures were characterized and analyzed by metallographic observation and scanning electron microscope. The effects of deformation temperature on the matrix structure, surface oxide and coating structure of hot-dip galvanized hot-formed steel were studied. Combined with the analysis results, the door anti-collision rod was trial-produced using galvanized hot-formed steel. The results show that the content of martensite in the matrix increases with the increase of deformation temperature. When the deformation temperature increases to 810°C, the matrix is full martensite. After hot stamping, the oxide layers of Zn, Fe, Mn and Al are granular and discontinuously distributed on the surface of the coating. The coating is composed of α-Fe(Zn) and Γ-Fe_3Zn_{10} phases, and the content of Zn in the coating increases with the increase of deformation temperature. When the deformation temperature is higher than the peritectic transformation temperature of α-Fe(Zn) + Γ-Fe_3Zn_{10} → α-Fe(Zn) + Zn_{liq}, the LMIE phenomenon occurs. The liquid Zn penetrates into the steel matrix and produces macroscopic cracks in the steel matrix. At the deformation temperature of 750°C, the stamping test of the parts is carried out. Only microcracks appear inside the coating, and the overall distribution of the coating is relatively uniform. The thickness range of the coating is 22-30μm.

Keywords: Galvanized hot-formed steel; Hot press forming; Microstructure; LME cracks.

1. Introduction

In recent years, under the general trend of global energy reduction and emission reduction, the automotive industry has an increasing demand for lightweight parts. 22MnB5 has good formability and hardenability. It can obtain ultra-high strength components with full martensite after forming and quenching. The tensile strength is more than 1500 MPa. It is often used in A/B pillar reinforcements, bumpers and other parts to ensure the safety of automobiles.[1-3] However, when high strength steel uses the traditional cold forming process, it is easy to have problems such as large springback, high impact load, large wear and reduce mold life. In contrast, the hot stamping process heats the steel plate to a high temperature state, followed by rapid stamping and quenching of the material, which not only takes advantage of the good formability of the material at high temperature but also ensures the service life of the mold. In particular, hot forming can produce ultra-high

Y. Zhang and M. Ma (eds.), *Proceedings of the 7th International Conference on Advanced High Strength Steel and Press Hardening (ICHSU 2024)*, Atlantis Highlights in Materials Science and Technology 3,
https://doi.org/10.2991/978-94-6463-581-2_49

strength parts with high dimensional accuracy and no springback with tensile strength exceeding 1500 MPa.[4-6] However, the material is prone to decarburization and oxidation peeling at high temperature, which affects the performance of the parts.[7] Therefore, the coating technology of hot forming steel is also constantly developing. For example, the most widely used coating is Al-Si coating, but Al-Si coating does not have cathodic protection performance, and it is easy to corrode at the incision of the part and reduce the durability of the part.[8] Zinc-based coating can solve the above problems. Because zinc has stronger electronegativity than iron, zinc coating can provide cathodic protection to steel substrate by sacrificing corrosion, which greatly improves the corrosion resistance of parts.[9]

In the process of hot stamping, Fe-Zn diffusion reaction occurs in zinc-based coating 22MnB5 steel. Kang et al.[10] studied the effect of annealing temperature on Fe-Zn reaction by heating galvanized 22MnB5 to 500-900°C for heat treatment. Hao Peng et al.[11] proposed a three-stage diffusion mechanism between Fe and Zn in the austenitizing process of galvanized 22MnB5 based on the fracture process of Fe_2Al_5 inhibition layer. The melting point of zinc is 419.5°C.There will be liquid zinc in the coating during hot stamping, which may lead to liquid metal induced brittle fracture (LMIE) and lead to early fracture of stamping parts, which also limits the application of galvanized hot stamping steel.[12] Many researchers have studied the microcrack formation mechanism of LMIE phenomenon. Lawrence Cho et al.[13] analyzed the microstructure of brittle cracks in liquid metal of galvanized 22MnB5 steel in detail, and proposed a new LME crack formation model of α-Fe(Zn) film at austenite grain boundary leading to grain boundary fracture embrittlement. RAZMPOOSH et al.[14] studied the role of grain boundary characteristics in liquid metal embrittlement, indicating that liquid metal penetration is determined by grain boundary misorientation angle and applied tensile stress couple.

Due to the simultaneous existence of stress and liquid zinc, the hot forming steel with zinc-based coating will produce the cracking problem of “liquid metal induced brittleness (LMIE)” during high temperature deformation. The deformation temperature is very important to eliminate the existence of liquid zinc. Therefore, this paper studies the influence of different deformation temperatures on the microstructure and coating structure of galvanized 22MnB5, in order to provide reference for the formulation of hot forming process of galvanized hot forming steel.

2. Material and methods

The experimental material is 1.4mm cold rolled galvanized 22MnB5 steel plate produced by a steel plant, and its major composition is shown in Table 1.

Table1. Chemical composition of the steel with Zn coating used in this study (mass weight,%).

C	Mn	Si	S	P	Fe
⩽0.15	⩽2.50	⩽0.8	⩽0.015	⩽0.08	Bal.

The hot stamping process of galvanized 22MnB5 steel was simulated by Gleeble 3800, and the sample temperature was detected by K-type thermocouple welded in the center of the sample surface. The simulated process system is shown in Fig.1. The sample was heated to 910°C at 10°C/s and held at this temperature for 300s, and then cooled to 720°C, 750°C, and 810°C to deform to a true strain of 0.25 at a strain rate of $0.1s^{-1}$. The sample is then immediately quenched to room temperature with compressed nitrogen. The longitudinal section of the uniform temperature zone of the sample was taken for subsequent analysis, and the sample was inlaid, ground and polished. The microstructure of the sample matrix was etched with 4% nitric acid alcohol solution, and the etching time was about 5s. The structure and composition of the coating were analyzed by ZEISS ULTRA55 field emission scanning electron microscope.

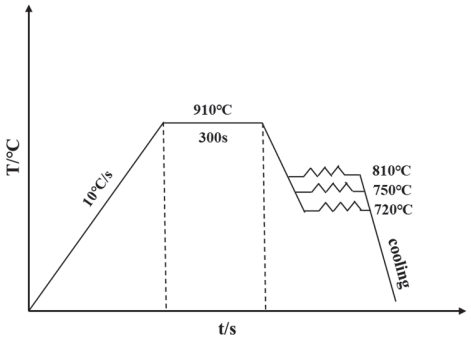

Fig.1. The schematic diagram of temperature system for simulating hot stamping process.

3. Results and discussion

3.1. *Structure morphology of the original plate*

Fig.2 is the matrix structure of the cold rolled sheet, which is composed of ferrite and pearlite. The coating microstructure and EDS results of galvanized hot forming steel sheet are shown in Fig.3. The original coating thickness of galvanized 22MnB5 steel plate is about 12.2 μm, which is composed of pure zinc and interface inhibition layer Fe_2Al_5.In order to inhibit the violent reaction between Fe and Zn, a certain amount of Al is added to the zinc pot to preferentially react with Fe to form Fe_2Al_5 interface inhibition layer, and the inhibition layer at the interface between the substrate and the coating is continuously distributed.

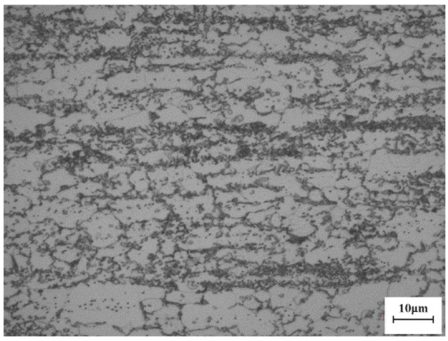

Fig.2. The matrix structure of cold rolled sheet.

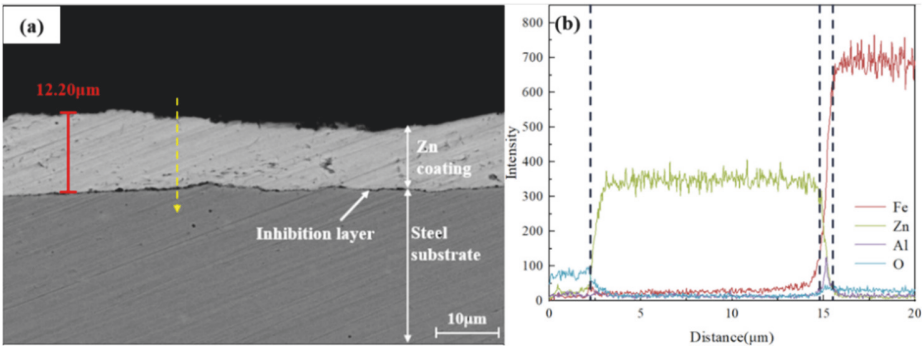

Fig.3. (a)The coating morphology and (b) line scan results of the original plate.

3.2. *Matrix microstructure evolution at different deformation temperatures*

The microstructure of 22MnB5 galvanized sheet substrate at three hot forming temperatures is shown in Fig.4. When the deformation temperature is 720°C, there are more ferrite and some martensite in the matrix structure. With the increase of deformation temperature, the content of martensite in the matrix structure increases, while the content of ferrite decreases. When the temperature reaches 810°C, the matrix is completely martensite.

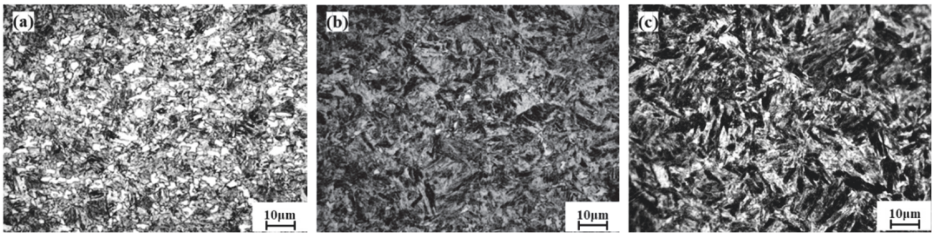

Fig.4. Microstructure images of matrix at different temperatures: (a) 720°C; (b) 750°C; (c)810°C.

3.3. *Analysis of surface oxides*

Fig.5 shows the SEM results of the coating surface at different deformation temperatures. The surface oxides of the samples were analyzed by EDS, and the point scanning results

are shown in Table 2. The morphology of the surface oxides at different deformation temperatures is not much different, and they are all granular and discontinuously distributed on the surface. There are cracks with a width of 5-10μm on the surface of the coating. According to the point scan results, the oxide particles with larger size of P1 and P4 contain more than 60% of Zn element, and it is speculated that the oxide is ZnO. The P2 point contains 42.03% Mn element, and the P5 point contains up to 54.09% Fe. It is speculated that the oxide is Fe2O3 or Fe3O4. In addition, according to the results of surface scanning and point scanning, the presence of Al element was also observed on the surface. The formation of surface oxides is mainly affected by the heating process and holding time. During the heating and holding process, the Zn element diffuses to the surface of the coating, gradually evaporates and oxidizes, and the inhibition layer is gradually destroyed. The Al element and the Fe element in the matrix are not limited. The Al element migrates to the surface to form Al2O3, and the surface oxide of the coating is further thickened. Finally, it is composed of ZnO, Al2O3, Fe and Mn oxides. The existence of the oxide layer avoids the further volatilization of Zn in the coating at high temperature.

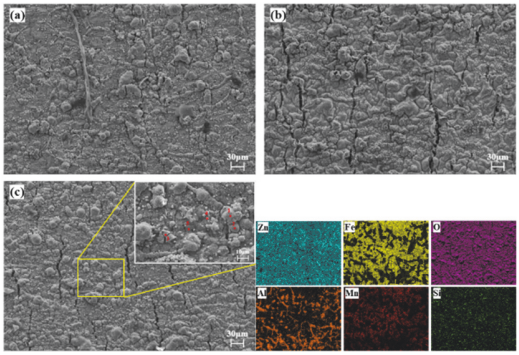

Fig.5. SEM micrographs and EDS of coating surface at different temperatures: (a) 720℃; (b) 750℃; (c) 810℃.

Table2. Measurement results of element content in EDS analysis for the specimen correspondig to Fig.5.

Point	Zn	Fe	O	Al	Mn	Si
P1	68.65	5.61	15.89	0.53	9.33	0.00
P2	38.19	3.81	15.77	0.12	42.03	0.08
P3	60.18	4.77	18.53	0.63	15.80	0.09
P4	60.74	4.89	22.34	1.38	10.33	0.33
P5	26.00	54.09	8.09	10.67	0.77	0.38

3.4. *Evolution of coating structure*

The SEM and EDS results of the coating structure at three different deformation temperatures are shown in Fig.6.Table 3 shows the EDS point scan results. Fig.6(a) and (b) show that the content of Zn in the coating at 720°C is 25-30%. When the deformation temperature increases to 750°C, the content of Zn in the coating increases to 30-38%. At 720°C and 750°C, the coating is mainly α-Fe(Zn) phase, and The concentrated area of Zn

element only exists near the surface of the coating. As shown in Fig.6(c), the content of Zn in the white phase of the coating is as high as 88.48% at 810°C. It can be determined that the white phase is Γ-Fe_3Zn_{10} phase, and the phase ratio is about 16%. The content of gray phase Fe in the coating is 76.15%, and the corresponding structure is α-Fe(Zn) phase, which accounts for about 84% in the coating. It is found that the crack extends to about 95.5μm in the steel matrix. According to the point scan results, the content of Zn element near the crack is as high as 88.95%, which can be judged as the crack caused by liquid metal brittleness (LME).

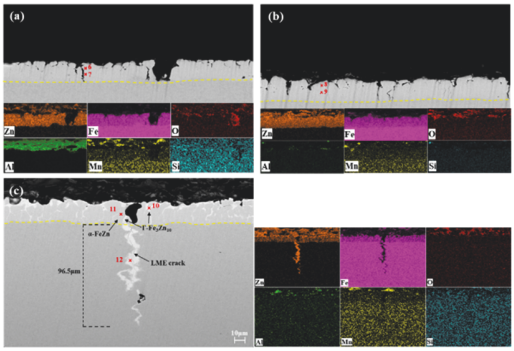

Fig.6. The SEM images and EDS surface scanning results of the coating structure at the deformation temperature of (a) 720℃; (b) 750℃; (c) 810℃.

Table3. Measurement results of element content in EDS analysis for the specimen corresponding to Fig.6.

Point	Zn	Fe	O	Al	Si
P6	28.09	71.05	0.58	0.27	0.00
P7	26.37	72.83	0.52	0.00	0.28
P8	37.61	61.52	0.87	0.00	0.00
P9	32.69	66.24	1.06	0.00	0.00
P10	88.48	10.88	0.63	0.00	0.00
P11	22.99	76.15	0.59	0.00	0.27
P12	88.95	9.76	1.01	0.00	0.28

According to the Fe-Zn binary phase diagram shown in Fig.7,[15] the gray area is the area where the LMIE crack is generated. When stamping at 810°C, the Zn content in Γ-Fe_3Zn_{10} phase is 88.48 %, and the deformation temperature is higher than the temperature of peritectic transformation α-Fe(Zn) + Γ-Fe_3Zn_{10} → α-Fe(Zn) + Zn_{liq}. Therefore, during the hot deformation process, part of Γ-Fe_3Zn_{10} is transformed into liquid Zn, resulting in the coating composed of α-Fe(Zn) and liquid Zn. The presence of liquid phase brittles the α-Fe (Zn) grain boundary. When tensile stress is applied, LMIE cracking is easy to occur at the solid-liquid interface, and liquid Zn continues to diffuse along the α-Fe (Zn) grain boundary to the austenite grain boundary of the matrix. As the deformation progresses, macroscopic cracks are formed in the steel matrix. When deformed at 720 °C and 750 °C, the temperature is lower than the peritectic transition temperature, and only microcracks are generated in the coating.

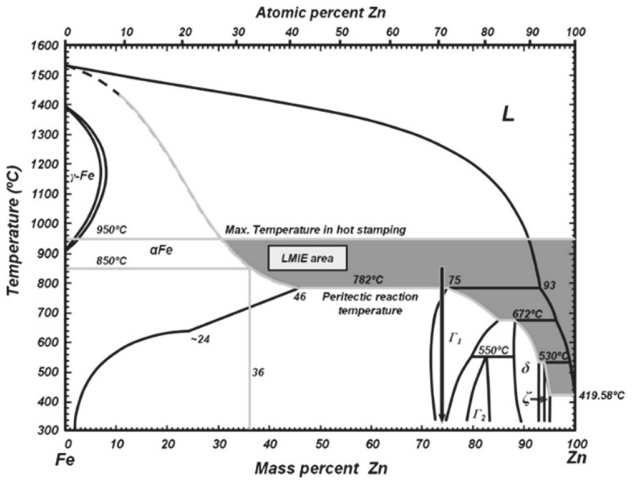

Fig.7. Fe-Zn phase diagram.

3.5. *Coating structure of trial parts*

By analyzing the thermal simulation results of Gleeble 3800, when the deformation temperature is 750°C, the matrix structure of the galvanized 22MnB5 plate is martensite, and there are only a few microcracks in the coating. Therefore, the stamping parts were trial-produced by the temperature system of 910°C holding 300s at 750°C deformation. Considering that the deformation force of the parts at different positions in the hot stamping process will also be different, the simulation analysis of the hot stamping process is first carried out to determine the stress distribution of each position of the parts. Fig.8(a) shows the strain distribution at each position of the part after stamping. It can be found that the strain value is the largest at the bending position of the part. Fig.8(c),(d),(e) shows the stress variation curves at different positions in the stamping process, where S11, S22 and S33 are the stress distribution in X, Yand Z directions. The positive value is expressed as tensile stress, and the negative value is expressed as compressive stress. The position of P1 is subjected to tensile stress in the two directions of S11 and S33 in the early stage of stamping, and then transformed into three-dimensional compressive stress in the later stage. The P2 position is continuously subjected to three-dimensional tensile stress during the stamping process, and the tensile stress continues to increase with the stamping process. The P3 position is subjected to three-dimensional compressive stress during the stamping process. In the stamping process, the tensile stress will promote the generation of coating cracks, while the compressive stress will inhibit the generation and propagation of cracks. [16-17] Therefore, combined with the stamping simulation results, the coating situation at the P2 position of the part can better represent the overall coating quality of the part. The observation position of the coating are shown in Fig.9.

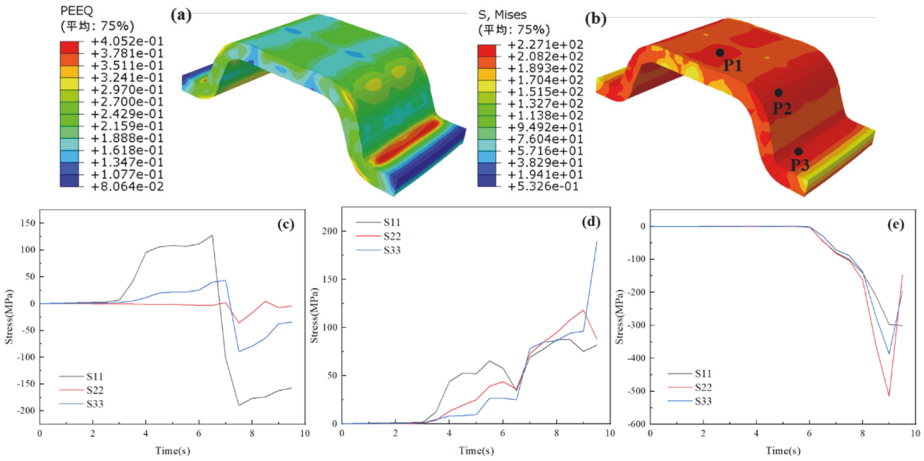

Fig.8. The (a)stress and (b)strain distribution of parts after stamping is completed. The curve of stress changing with time in the stamping process of (c)P1,(d) P2and (e) P3.

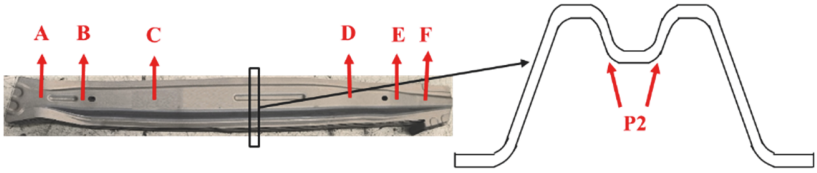

Fig.9. Coating observation position of trial parts.

Fig.10 is the SEM and EDS results of the coating on the P2 position of the hot stamping parts. The thickness of the coating at the bending position is 22.67μm, and there are only microcracks inside the coating. This is because under the action of stamping tensile stress, microcracks are generated at the grain boundary of α-Fe(Zn). Because there is no liquid Zn in the coating, microcracks only propagate in the coating. In addition, due to the complex stress state at the bending point, it is also possible to cause micro-cracks due to the influence of tensile strain and friction. According to the energy spectrum results in Table 4, the Zn content in the coating is about 35%, so the coating is dominated by α-Fe(Zn) phase. According to the scanning results of Zn in Fig.10, there is a small amount of Γ-Fe_3Zn_{10} phase near the surface of the coating.

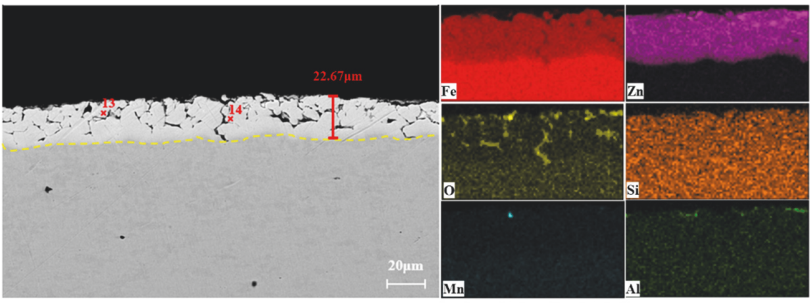

Fig.10. SEM images of coating on trial parts.

Table3. Measurement results of element content in EDS analysis for the specimen corresponding to Fig.10.

Point	Zn	Fe	O	Al	Si
P13	34.88	55.12	9.78	0.00	0.22
P14	34.15	54.52	10.96	0.00	0.37

Fig.11 shows the morphology and thickness of the coating in the transverse position of the hot stamping parts. The coating of the parts is relatively uniform, and the thickness of the coating is between 22-30μm. There are some micro-cracks in the coating, which do not extend to the steel matrix.

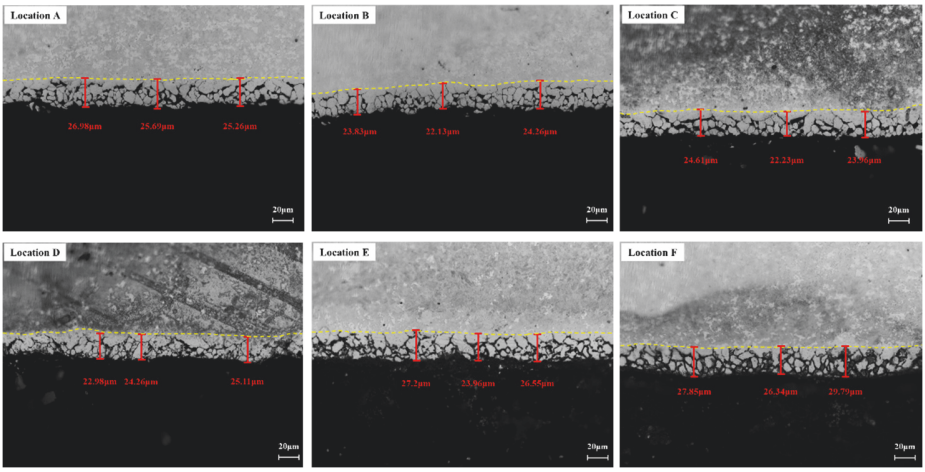

Fig.11. Coating morphology of trial parts.

4. Conclusions

Through the study of 22MnB5 galvanized steel sheet at different stamping temperatures, the influence of deformation temperature on the matrix structure and coating structure was obtained.

1) When the deformation temperature is 720°C, there is a large amount of ferrite in the matrix of the sample. With the increase of deformation temperature, the martensitic transformation is more sufficient. When the temperature is increased to 810°C, the matrix structure has been completely transformed into martensite.

2) The original coating is pure zinc phase, and there is a Fe_2Al_5 inhibition layer between the coating and the steel substrate. After hot stamping, the surface of the coating is covered with Fe, Zn, Al and Mn oxide layers, and the coating is composed of α-Fe(Zn) and Γ-Fe_3Zn_{10} phases.

3) When the deformation temperature is higher than the peritectic transformation temperature of α-Fe(Zn) + Γ-Fe_3Zn_{10} → α-Fe(Zn) + Zn_{liq}, there is liquid Zn in the coating of galvanized 22MnB5 steel, which is easy to produce LME macroscopic cracks during hot stamping.

4) The overall coating of the stamping trial parts is evenly distributed at 750°C, and the thickness of the coating is between 22-30μm, and only some microcracks exist in the coating.

Acknowledgments

Authors acknowledge the financial support from Shijiazhuang Science and Technology Bureau for the major science and technology projects of universities stationed in Hebei (241080457A).

References

1. Zhuang W , Wang P , Xie D ,et al.Experimental study and a damage model approach to determine the effect of hot forming deformation on the service performance of 22MnB5 steel.Journal of Manufacturing Processes, 2019, 47(Nov.):10-21.
2. Güler H, Ertan R, Özcan R. Investigation of the hot ductility of a high-strength boron steel. Materials Science and Engineering: A, 2014, 608: 90-94.
3. Zhu L, Gu Z, Xu H, et al. Modeling of microstructure evolution in 22MnB5 steel during hot stamping. Journal of Iron and Steel Research International, 2014, 21(2): 197-201.
4. Zhuang W , Wang P , Xie D ,et al.Experimental study and a damage model approach to determine the effect of hot forming deformation on the service performance of 22MnB5 stee.Journal of Manufacturing Processes, 2019, 47(Nov.):10-21.
5. Bok H H, Lee M G, Pavlina E J, et al. Comparative study of the prediction of microstructure and mechanical properties for a hot-stamped B-pillar reinforcing part. International journal of mechanical sciences, 2011, 53(9): 744-752.
6. Xiaodong L I , Shuo H , Cunyu W ,et al. Research on the warm-hot forming process and its performance evaluation for the third-generation automobile steel. Journal of Mechanical Engineering, 2017, 53(8): 35-42.
7. Kondratiuk J, Kuhn P, Labrenz E, et al. Zinc coatings for hot sheet metal forming: Comparison of phase evolution and microstructure during heat treatment. Surface and Coatings Technology, 2011, 205(17-18): 4141-4153.
8. Manzenreiter T, Rosner M, Kurz T, et al. Challenges and advantages in usage of zinc-coated, press-hardened components with tailored properties. BHM Berg-und Hüttenmännische Monatshefte, 2012, 3(157): 97-101.
9. Okamoto N L , Kashioka D , Inomoto M , et al.Compression deformability of Γ and ζ Fe–Zn intermetallics to mitigate detachment of brittle intermetallic coating of galvannealed steels.Scripta Materialia, 2013, 69(4):307-310.
10. Kang J H, Kim D, Kim D H, et al. Fe-Zn reaction and its influence on microcracks during hot tensile deformation of galvanized 22MnB5 steel. Surface and Coatings Technology, 2019, 357: 1069-1075.
11. Peng H, Peng W, Lu R, et al. Diffusion and cracking behavior involved in hot press forming of Zn coated 22MnB5. Journal of Alloys and Compounds, 2019, 806: 195-205.
12. Mendala J, Liberski P. Liquid metal embrittlement of steel with a coating obtained by batch hot dip method in a Zn+ 2% Sn bath. Solid State Phenomena, 2014, 212: 107-110.

13. Cho L, Kang H, Lee C, et al. Microstructure of liquid metal embrittlement cracks on Zn-coated 22MnB5 press-hardened steel. Scripta Materialia, 2014, 90: 25-28.
14. Razmpoosh M H, Macwan A, Goodwin F, et al. Role of random and coincidence site lattice grain boundaries in liquid metal embrittlement of iron (FCC)-Zn couple. Metallurgical and Materials Transactions A, 2020, 51: 3938-3944.
15. Lee C W, Fan D W, Sohn I R, et al. Liquid-metal-induced embrittlement of Zn-coated hot stam** steel. Metallurgical and Materials Transactions A, 2012, 43: 5122-5127.
16. LI Xue-tao, ZHU Guo-sen, MA Wen-yu. et al. The crack generation, propagation mechanism and thermal property of Zn-coated hot stamping steel.Journal of Central South University,1-17.
17. Razmpoosh M H, Langelier B, Marzbanrad E, et al. Atomic-scale investigation of liquid-metal-embrittlement crack-path: revealing mechanism and role of grain boundary chemistry. Acta Materialia, 2021, 204: 116519.